Subcluster merging in clusters of galaxies and the cosmological density parameter

F. E. Nakamura[1], M. Hattori[2], and S. Mineshige[1]

[1] Department of Astronomy, Faculty of Science, Kyoto University, Sakyo-ku, Kyoto 606-01, Japan
[2] Max-Planck-Institut für Extraterrestrische Physik, D-85740 Garching, Germany

Abstract. Recent X-ray observations have established that collisions between subclusters of galaxies are rather common phenomena. Prompted by such observations, we have performed N-body simulations of two equal-mass subclusters of galaxies, which are going to merge. We first have confirmed that only a part of kinetic energy associated with the relative motion of two subclusters is converted to internal energy of each subcluster at the first encounter. Two subclusters, therefore, once pass through each other, turn around due to gravitational attraction, and finally merge at the second or third encounter. We performed simulations for a variety of dark-matter (DM) distributions, and find that the time scale for washing out the double peak structures after the first encounter strongly depends on the distribution of the density and velocity distributions of the DM. It takes longer when the DM is spatially extended and/or when the velocity distribution of the DM has a Gaussian shape, rather than a uniform distribution. According to our calculation it takes more than 4×10^9yr after the first encounter until the density contour shows only a single peak.

To explain the high fraction of the clusters with substructures among nearby clusters, Richstone,Loeb & Turner(1992; hereafter RLT) required recent($\sim 10^9 h^{-1}$yr) cluster formation. However, our results show that the timescale for subcluster merging is still uncertain and possibly much longer than the time scale assumed by RLT. Caution should be exercised when concluding that the density of the universe is high by using RLT's method.

Key words: Galaxies: clustering – dark matter – large-scale structure of Universe

1. Introduction

The existence of double or multiple peaks in the spatial mass distribution has been established for a number of clusters of galaxies. Jones & Forman (1990), for example, have reported that about 30 % of 250 clusters of galaxies have double or multiple peaks in the X-ray surface brightness. Since the X-ray emissivity is more sensitive to the density rather than to the temperature, their observations strongly indicate the presence of multiple peaks in the distribution of the intracluster medium (ICM). ROSAT observations of the clusters of galaxies have established that the high fraction of the galaxy clusters have double or multiple peaks in the distribution of the X-ray emitting gas (e.g. Briel et al. 1991). The existence of such double or multiple peaks has been also known for the galaxy distribution in $\sim$ 40 % of 40 clusters of galaxies (Geller & Beers 1982). Moreover, Miralda-Escudé (1991) has recently inferred from the analysis of the gravitational lensing clusters that the distribution of the gravitational mass, that is the mass of the all constituents including dark matter, in the clusters of galaxies is not spherically symmetric, but has multiple peaks. These observations of the distribution of ICM, galaxies and dark matter in clusters suggest frequent occurrence of merger events between subclusters in clusters of galaxies.

Frequent collisions between subclusters are of great importance for measuring the geometry of the universe. Regarding the presence of substructuring as a signature of recent cluster formation, RLT estimated the lower limit to the cosmological density parameter to be $\Omega_0 \gtrsim 0.5$. This is a rather large value and is in contradiction with the results deduced from the another methods (e.g. Briel et al. 1991; Yoshii & Takahara 1989). For example, the local estimates of the cosmological density parameter, the baryon fraction in individual objects (e.g. Briel et al. 1992; White et al. 1993) and the results from the peculiar velocity field (e.g. Tully 1987), and deep galaxy number counts (Yoshii & Takahara 1989) support a low density universe. We thus

need to re-examine the basic assumptions made by RLT and check the significance of their obtained result.

Their fundamental assumptions are: (1) the initial perturbations are comoving with the Hubble flow, (2) the shape of the initial perturbations is spherically symmetric, and (3) the relaxation timescale, τ_{relax}, on which multiple structures within a cluster is erased after the gravitational collapse of the cluster, is at most a cluster crossing time, of the order of $\sim 10^9 h^{-1}$ yr. The first and second assumptions have been checked by Bartelmann et al. (1993). They introduced initial velocity fluctuation and non-spherical perturbation to find that RLT's conclusion gets firmer by these additional and more realistic conditions.

However, the third assumption seems to be more crucial for RLT's argument since the lower limit of the cosmological density parameter obtained by RLT's method is rather sensitive to the assumed relaxation time will be shown in Sec.4. McGlynn & Fabian (1984, hereafter MF) have shown that it takes more than several crossing times after the first encounter of the substructures to erase multiple structures after the first encounter of the substructures unless a strong two body relaxation works during the collision.

In the present study, we perform extensive studies of subcluster merging, following the line of MF, but adopting more general conditions for the initial spatial and velocity distributions for the DM in clusters. In fact, the relaxation time depends strongly on these distributions and the spatial distribution of the DM is still largely uncertain (see Sec.2.2). Using the simulation results, we investigate how the constraint on the cosmological density parameter using RLT's method is relaxed. In Sect. 2 we briefly describe our model. The results of N-body simulations are presented in Sect. 3. The final section is devoted to summary and discussion.

2. Models

2.1. Basic assumptions

We investigate the merging of two virialized subclusters as an example for substructure within an unrelaxed cluster of galaxies. We use the same model parameters as MF to enable a direct comparison (see Table 1). Two subclusters with equal total masses are assumed, since the size of substructure is comparable to that of the main structure in about half of the observed clusters (Dressler & Shectman 1988). Particle number (N) of each cluster is 1024, 20 % of which are assumed to be galaxies and the remaining 80 % to DM. The mass of a dark-matter particle, m_{DM}, is 100 times larger than the mass of a galaxy particle, m_{gal}.

Here we assume that the gravitational force of the ICM is negligible for the evolution of the cluster.

Table 1. Standard model parameters. N represents the total number of galaxy or DM particles, M is the total mass of one subcluster, and m is a mass of one galaxy or DM particle. Indices DM and gal represent the dark matter and the galaxy component, respectively.

Particles (N)	1024×2
Total mass (M)	$(8 \times 10^{14} M_\odot) \times 2$
$N_{\mathrm{DM}}/N_{\mathrm{gal}}$	4
$m_{\mathrm{DM}}/m_{\mathrm{gal}}$	100
$M_{\mathrm{DM}}/M_{\mathrm{gal}}$	400

2.2. Initial mass distributions in each cluster

It is observationally known that the galaxy distribution in compact clusters is well approximated by the isothermal King distribution (King 1972),

$$\rho_{\mathrm{gal}} = \frac{\rho_{\mathrm{gal}}^0}{\left[1 + (r/r_{\mathrm{gal}})^2\right]^{3/2}}, \tag{1}$$

where ρ_{gal}^0 is the central density and r_{gal} is the core radius for the galaxies in the cluster (Sarazin 1988). According to Bahcall (1975), we fix the core radius to $r_{\mathrm{gal}} = 250$ kpc in the present studies. The central density ρ_{gal}^0 is defined by $\int 4\pi \rho_{\mathrm{gal}}(r) r^2 dr = M_{\mathrm{gal}}$, where M_{gal} is the total mass of the galaxies in the cluster (Table 1). Since this integral diverges $M_{rmgal} \sim \ln r$ at large r, we truncate the distribution at $r_{\mathrm{max}} = 5 r_{\mathrm{gal}}$, which is 1.25 Mpc for $r_{\mathrm{gal}} = 250$ kpc.

Unlike the galaxy distribution, the DM distribution is still under discussion (Hughes 1989; Fitchett 1990). We hence adopt the following parameterization in analogy with the gas distribution in the cluster (Cavaliere & Fusco-Femiano 1976);

$$\rho_{\mathrm{DM}} = \frac{\rho_{\mathrm{DM}}^0}{\left[1 + (r/r_{\mathrm{DM}})^2\right]^{3\alpha/2}} \tag{2}$$

where the core radius, r_{DM}, and the slope, α, of the DM distribution are free parameters. The adopted parameters are summarized in Table 2. A constant ρ_{DM}^0 is determined so that $M_{\mathrm{DM}} = \int 4\pi \rho_{\mathrm{DM}}(r) r^2 dr$. The combined X-ray and optical study of the mass distribution in the Coma cluster (Hughes 1989) has shown that the mass-follows-light models are the most precise to date, i.e. $r_{\mathrm{DM}} = r_{\mathrm{gal}}$ and $\alpha = 1$ in our notation. The study of the distribution of the dark matter in the A2256 (Henry et al. 1993) has shown, on the other hand, that the mass-follows-gas models, i.e. flatter distribution with $\alpha \sim 2/3$, is also consistent with the present X-ray observations. A steeper mass distribution than the galaxy distribution, i.e. $\alpha \sim 4/3$, has not

Table 2. Adopted parameters for the structure of a subcluster and the resultant rebounce times (1 Gyr = 10^9yr). The first column is the model names. $\rho(r)$ is the density distribution of the DM. MK, IK and PL represent the modified King, the isothermal King and the power-law density distributions, respectively. α is the slope of the density profile. $r_{\rm DM}/r_{rmgal}$ is the core radius of the DM distribution in unit of the core radius of the galaxy distribution. $f(v)$ is the velocity profile of the DM. G and U represent the Gaussian distribution and uniform distribution, respectively. The initial relative velocity is given by Eq. (5), except for Model J, in which $V_{\rm ini} = 0$. The core radius for galaxies, $r_{\rm gal}$, is taken to be 250 kpc, while $R_{\rm ini} = 3.125$ Mpc in all models.

Model	$\rho(r)$	α	$r_{\rm DM}/r_{\rm gal}$	$f(v)$	$\tau_{\rm reb}$(Gyr)
A	MK	2/3	0.1	G	9.0
B	MK	2/3	1.0	G	8.0
C	MK	2/3	3.0	G	9.5
D	IK	1	0.1	G	7.0
E	IK	1	1.0	G	8.5
F	IK	1	3.0	G	10.5
G	MK	4/3	0.1	G	6.0
H	MK	4/3	1.0	G	7.5
I	MK	4/3	3.0	G	9.0
J	MK	4/3	0.1	G	4.0
M_0	PL	(2/3)	(0.0)	U	7.0
M_1	PL	(2/3)	(0.0)	G	11.0

been rejected either (Hughes 1989; Ponman 1992). Further more, much smaller core radii for the DM distribution in rich cluster than the core radii of the luminous components are inferred from the mass distribution measurements using the gravitational lensing techniques; the high rate of finding arc-like structures (Le Favre et al. 1994; Wu & Hammer 1993) and the geometrical study of the giant luminous arcs in distant clusters (e.g. Hammer 1991; Miralda-Escudé & Babul 1994; Wu 1994). For comparison, we also performed a simulation with a large core radius, i.e. $3 \times r_{\rm gal}$. Note that MF adopted a power-law density profile

$$\rho_{\rm DM} = \rho_{\rm DM}^0 \left(r/r_{\rm gal}\right)^{-2}, \tag{3}$$

corresponding to a profile with $r_{\rm DM} = 0$ and $\alpha = 2/3$ in our notation.

We assume two different velocity distributions: One is a Gaussian distribution with a cut-off at the velocity of $V = \pm 4\sigma$. σ is determined by the condition that the initial system is virialized. The second one is a uniform velocity distribution, from $V = 0$ to $V = V_{\rm max}$, where $V_{\rm max}$ is determined by the condition that the initial system is virialized. The latter one was used by MF. The adopted parameters of all the calculated models are summarized in Table 2.

2.3. Time evolutionary calculations of subclusters

In a flat universe, the maximum expansion radius of perturbations which collapse at a redshift z_c in a $\Omega_0 = 1$ universe is expressed as

$$\ell_{\rm max} = 6.0 M_{15}^{1/3}(1 + z_c)^{-1}h^{-2/3}{\rm Mpc}, \tag{4}$$

where M_{15} is the mass of the perturbation in units of $10^{15}{\rm M_\odot}$. For $z_c \sim 1.0$ ($\sim 4.0 \times 10^9 h^{-1}$ yr from now in a critical density universe and even more in a low density universes), we find $\ell_{\rm max} \sim 3.0 h^{-2/3}$ Mpc. If $\Omega_0 < 1$ or $h < 1$, the maximum expansion radius of the clusters which collapsed at $z_c = 1$ is larger than the above value. The initial separation of two clusters is set to be $R_{\rm ini} = 2.5 \times r_{\rm max}(= 3.125$ Mpc) in all our models. Zero initial relative velocity with respect to the center of mass of the system , $V_{\rm ini} = 0$ (model J), corresponds to a collapse earlier than $z_c = 1$. Larger $V_{\rm ini}$ correspond to the case of the larger maximum expansion radius, i.e. a later collapse.

In all our calculations, except for model J,

$$\begin{aligned} V_{\rm ini} &= \sqrt{\frac{2GM}{R}} \\ &\simeq 1700({\rm km/s}) \left(\frac{M}{8 \times 10^{14}{\rm M_\odot}}\right)^{1/2} \left(\frac{R_{\rm ini}}{3{\rm Mpc}}\right)^{-1/2}. \end{aligned} \tag{5}$$

This is derived from the condition that two clusters were at rest at infinity. The crossing timescale, except for model J, is then approximately

$$\begin{aligned} t_c &\equiv R_{\rm ini}/V_{\rm ini} \\ &= 1.0 \times 10^9 \left(\frac{M}{8 \times 10^{14}{\rm M_\odot}}\right)^{-1/2} \left(\frac{R_{\rm ini}}{3{\rm Mpc}}\right)^{3/2}{\rm yr}. \end{aligned} \tag{6}$$

The gravitational force is calculated by direct summation. We use softening parameter of $\epsilon = 0.6$ Mpc. It has been shown (see p36-38 in Sarazin 1988) that the dark matter cannot be bound to individual galaxies but rather must form a continuum to prevent clusters from over relaxation due to dynamical friction. In other words, the two-body relaxation timescale in clusters is much longer than the timescale of a merger. Therefore the merging of clusters is treated as a collisionless process and we took a large value of $\epsilon = 0.6$Mpc which saves a lot of computating time.

The Equations of motion of particles are integrated by the 4-th order Runge-Kutta method. To examine the stability of the initial cluster configurations, we calculate the evolution of a single cluster for several crossing times (Eq. (6)), confirming no appreciable structural changes. The energy is conserved within 3% of the total energy in the every calculation.

## 3. Simulations

3.1. General behavior

We first calculate models with $\alpha = 2/3$, the same density profile as those of MF, $\rho_{\rm DM} \propto r^{-2}$ at $r \gg r_{\rm gal}$. The core radius is assumed to be $r_{\rm DM}/r_{\rm gal} = 0.1, 1.0$, and 3.0, for models A, B, and C, respectively (see Table 2), and the initial velocity is given by Eq. (5). Figure 1[1] shows a three-dimensional distribution of the DM particles for model B. Two clusters pass through each other, turn around due to mutual attraction, and recollide.
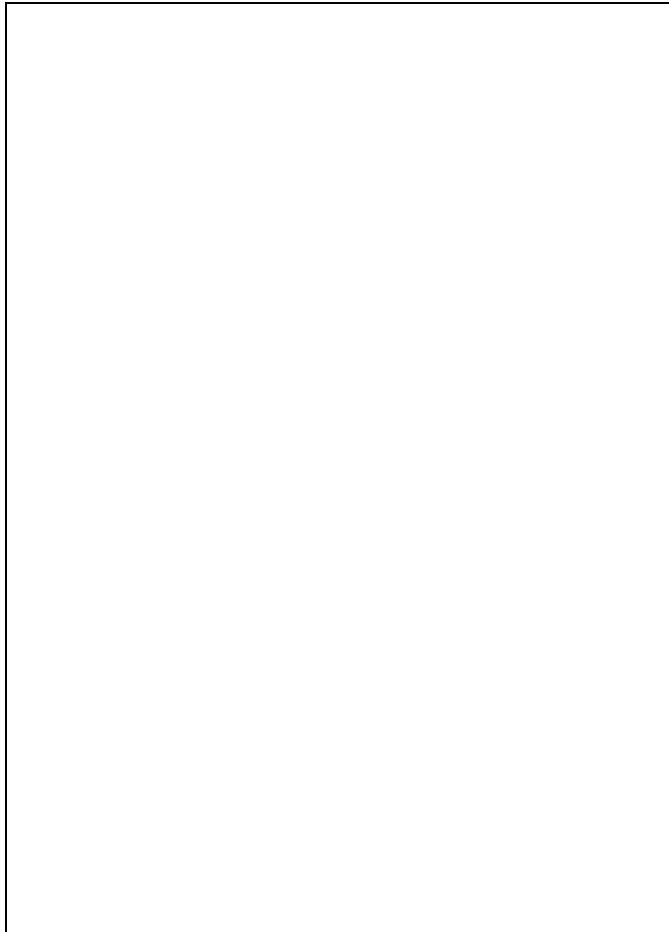
Fig. 1. Three-dimensional distribution of the DM particle positions for model B. The size of the box is 3 Mpc × 3 Mpc × 8 Mpc. The elapsed times in unit of t_{rmcr} are, from top to bottom, $t = 0.0, 1.6, 3.2$, and 4.8 in the left panel, and $t = 6.4, 8.0, 9.6$, and 11.2 in the right panel.

The upper panel of Fig. 2 illustrates the time variations of the distance of the center of mass of the two clusters in units of the crossing time, $t_{\rm cr}$ (Eq. (6)). The lower panel of Fig. 2 displays the half-mass radius of the DM in a cluster evolving with time, which is a rough indicator of the kinetic energy associated with the internal

---

[1]   The number of particles in Fig. 1 is reduced for the sake of saving the size of PS file in this online preprint.

motion. The half-mass radius increases right after the encounter. This indicates that the energy associated with the relative motion of the clusters is partly transferred into internal energy within the clusters during the first encounter. Nevertheless, further encounters are necessary to damp the oscillating motions of two subclusters completely, by forming a big cluster.
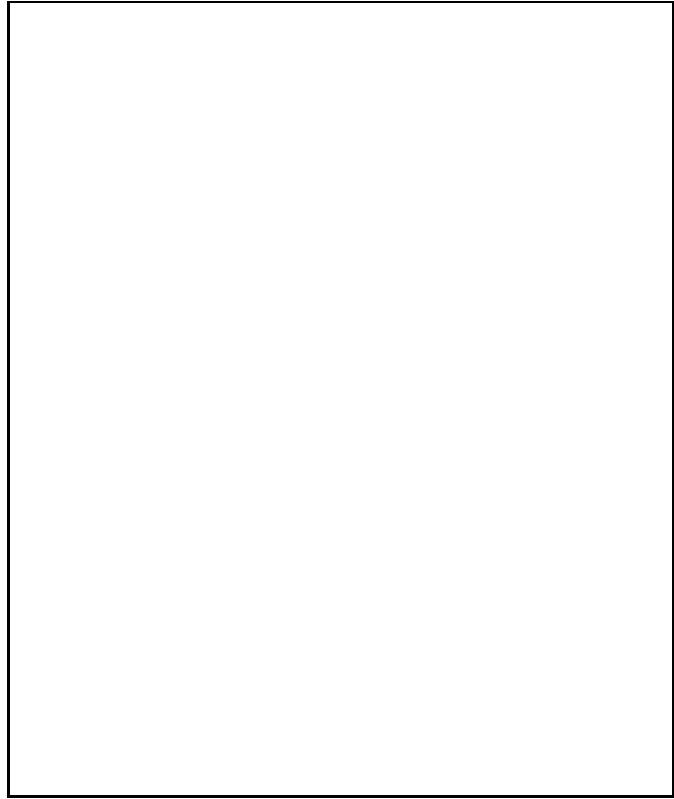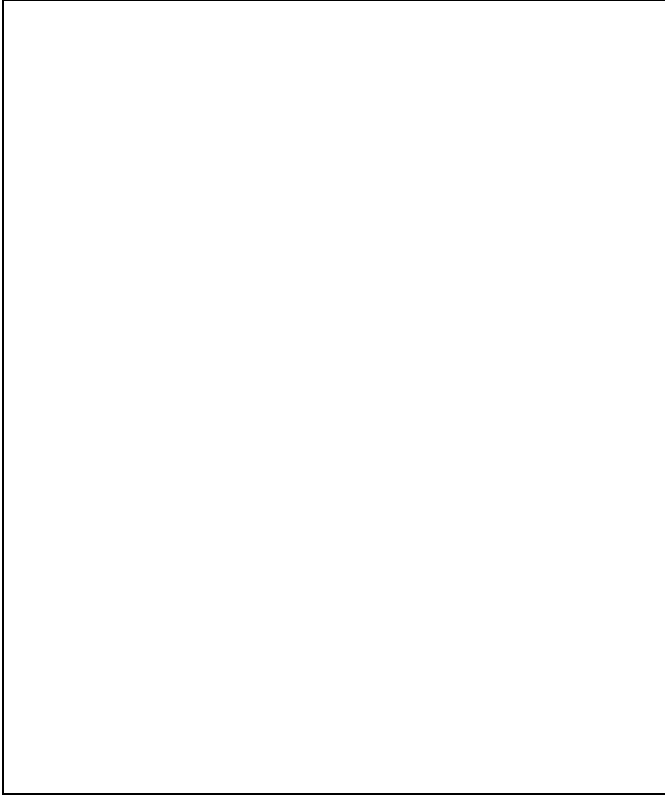

Fig. 2. The relative distance between the centers of the DM distributions of the two subclusters (the upper panel) and in the half-mass radius of the DM in one cluster (the lower panel) for models with $\alpha = 2/3$ versus time. In both panels, the solid line corresponds to the model with $r_{\rm DM} = 3r_{\rm gal}$, the dotted line to $r_{\rm DM} = r_{\rm gal}$, and the dashed line to $r_{\rm DM} = 0.1r_{\rm gal}$, respectively. The units of time and distance are $t_{\rm c}$ (Eq. (4)) and 1 Mpc, respectively.

Our main aim of this paper is to investigate the question how long the bimodal structure is preserved after the gravitational collapse of the cluster. The time of the first encounter of two substructures in our simulations corresponds to the cluster collapse. Since at least two encounters are necessary to wash out the bimodal structure in our all simulated models, the time interval between the first and second encounter, which we define as the rebounce time, gives a lower limit to the merging time-scale after the gravitational collapse. The resultant rebounce times are summarized in Table 2. We see that it is insensitive to the core radius of the DM in the models with $\alpha = 2/3$.

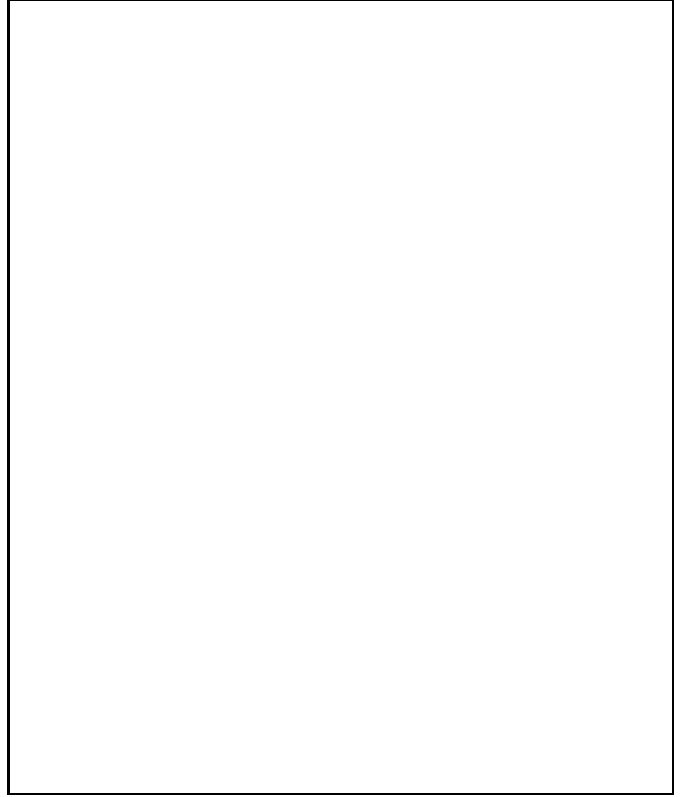## 3.2. Comparison with MF

For comparison with the results of MF, we performed similar simulations in model M_0. The density profile is power-law (Eq. (3)) (corresponding to the models with $\alpha = 2/3$ and $r_{DM} = 0$) and the velocity distribution of the DM is uniform. Figure 3 displays the distance of the two subclusters and the half-mass radius, respectively, as a function of time. The rebounce time of model M_0 is 7×10^9yr. Since the time unit defined in MF corresponds to 3×10^9yr in our models, this rebounce time corresponds to 2.3 in MF's time units. This is similar to the rebounce time of model A in MF which is the most similar to our models. Therefore, our simulation code could well reproduce MF's results.

Fig. 4. The same as Fig. 2 but for $\alpha = 1$.

3.3. Models with $\alpha = 1$ and $4/3$

In models with steeper density profiles, the rebounce time is rather sensitive to the core radius. Figure 4 is the same as Fig. 2 but for models with $\alpha = 1$; the solid line represents a model with $r_{DM} = 3r_{gal}$, the dashed line a model with $r_{DM} = 0.1r_{gal}$. The rebounce time responds with the core radius much more than the case with $\alpha = 2/3$; t_{reb} is reduced by a factor of 1.5, when we decrease r_{DM} by one order of magnitude. A similar trend can be seen for the case of $\alpha = 4/3$ (see Table 2). The core-radius dependence becomes weaker as α increases.

3.4. Bound models: dependence on V_{ini}

As discussed in Sect. 2.3, the case of the zero initial relative velocity correspond to the case in which the cluster collapses at earlier than $z_c = 1$. To demonstrate that multiple-peak structures still persist in the present mass distribution even if clusters collapsed at such an early epoch, we calculate a model with $V_{ini} = 0$. Since the rebounce time of model G is the shortest among our calculated models, we set the same initial conditions as model G except V_{ini} in model J. The rebounce time for models with $V_{ini} = 0$ but with other combinations of α and r_{DM} should be longer than the result of model J.

The time variation of the separation is illustrated in Fig. 5. Clearly, the rebounce time decreases by a ~ 30 %,

Fig. 3. The same as Fig. 2 but for the models without cores. The dotted line corresponds to MF's original model with a flat velocity profile (model M_0), while the solid line represents the model with the Gaussian velocity distribution (model M_1)

To investigate the effect of velocity distribution of the DM, a more realistic velocity distribution, a Gaussian distribution, is used in M_1, that is the Gaussian distribution. The rebounce time is about 1.5 times longer than MF's model M_0.

Fig. 5. The same as upper panel of Fig. 2, but for $\alpha = 4/3$ and $r_{DM}/r_{gal} = 0.1$. The dashed and solid lines represent the case with non-zero and zero initial velocity, respectively. The unit of time is 10^9yr.
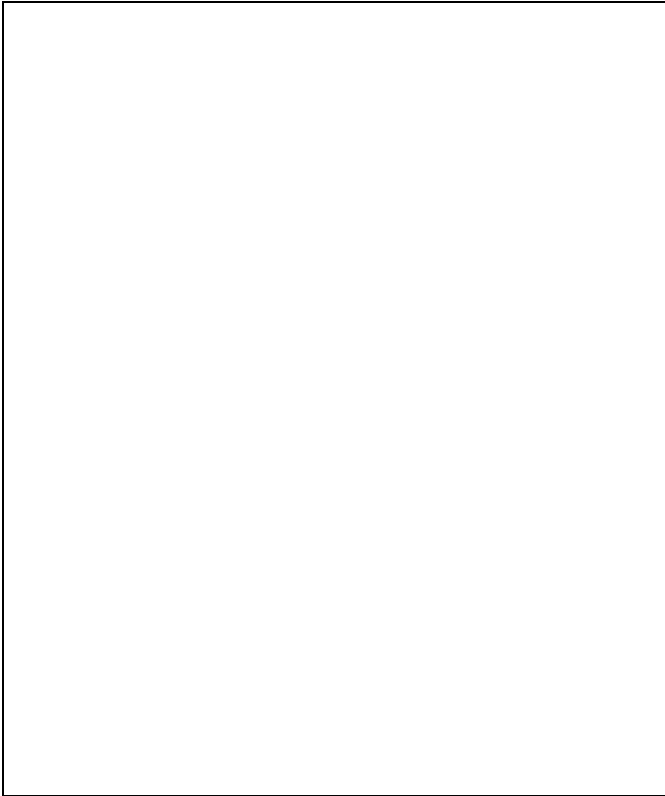
Fig. 6. Density distribution of some calculated models. The upper panels shows models with $\alpha = 2/3$ together with model M0, while the lower panels shows models with $\alpha = 4/3$. In both panels, the solid line corresponds to the case with $r_{DM} = 3r_{gal}$, the dotted line $r_{DM} = r_{gal}$, the dashed line $r_{DM} = 0.1r_{gal}$, and the dash-dotted line M0, respectively.

however, still it is factor $4h$ longer than the relaxation time assumed by RLT, that is $10^9 h^{-1}$yr. Further oscillatory motion with an amplitude of 1Mpc still remains after the second encounter. This result shows that we do not have to require the recent formation of nearby clusters with substructures as RLT did, where they assumed the sub-structuring clusters have collapsed within $10^9 h^{-1}$yr from now.

3.5. Interpretation of the results

Here we try to give the physical interpretations of the above results. As noted in Sect. 2.3, the two-body relaxation is not effective for subcluster mergers. Instead, violent relaxation, an energy exchange through variations of the potentials, plays a dominant role. The efficiency of the energy conversion then critically depends on how the potential changes with time, which, in turn, depends on the precise DM distribution in the cluster. The specific energy of a particle, $e = v^2/2 + \phi$, varies as

$$\frac{de}{dt} = v\frac{dv}{dt} + \frac{\partial\phi}{\partial t} + v\nabla\phi = \frac{\partial\phi}{\partial t}, \tag{7}$$

where v is the velocity of a particle, ϕ is the gravitational potential, and we used equation of motion, $dv/dt = -\nabla\phi$ (Lynden-Bell 1967). During the subcluster collisions, moreover, we may approximate as $\partial\phi/\partial t \simeq (\partial\phi/\partial x)v$. That is, the steeper is the potential curve, the quicker proceeds the merging process due to an efficient energy conversion.

In Fig. 6 we illustrate the density profiles of some calculated models, whereas Fig. 7 displays a potential of each model cluster. For the same core radius, say, $r_{DM}/r_{gal} = 0.1$, the potential curve is steeper, when α is larger, so that the relaxation time becomes shorter for models with larger α values. When a cluster has a relatively large core radius, r_{DM}, however, differences in potential curves are not significant, which explains why t_{reb} does not change in models with $r_{DM}/r_{gal} = 1.0$ or 3.0.

Likewise, for the same α values, say, $\alpha = 4/3$, the potential curve is steeper, when r_{DM} is smaller. The relaxation time is thus a decreasing function of the core radius when $\alpha = 1$ or $4/3$. In the models with $\alpha = 2/3$, on the other hand, this tendency is not clear, because the potential gradients do not differ so much from each other.

We also anticipate that the relaxation time is shorter, when the fraction of high-velocity particles is large. Funato et al. (1992) have shown that particles with initially higher energy get more energy than initially lower energy particles during the so called violent relaxation process. In this sense, a flat velocity distribution is favoured than the Gaussian distribution in terms of triggering a rapid relaxation. The distinction between models M_0 and M_1 is thus explained.
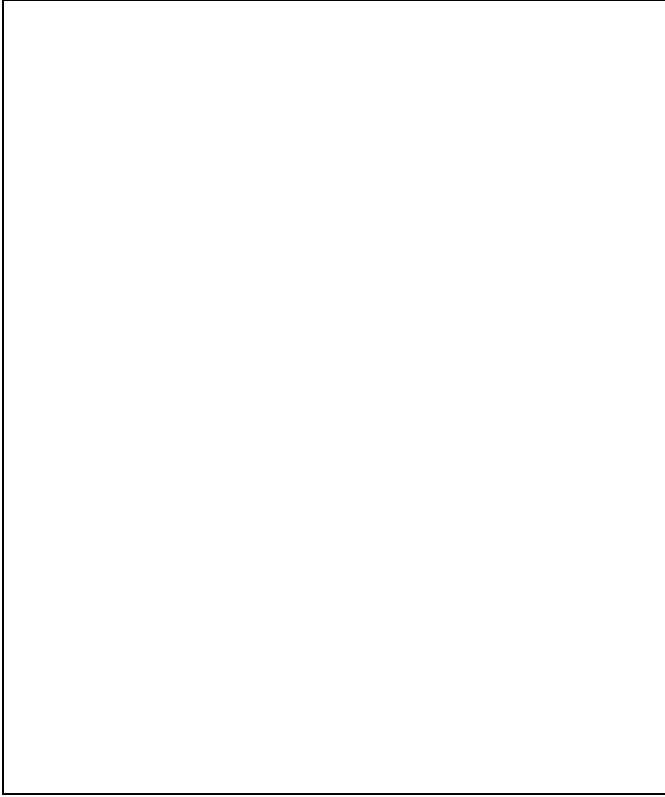
Fig. 7. Gravitational potentials generated by one cluster for each mass distribution model. Lines are same as Fig. 2.

3.6. Non-central collisions

So far only head-on collisions of subclusters were considered. We have also performed the simulations for an impact parameter $b = 250$ kpc. We find an even longer rebounce time than in central collision. This can be explained as follows: For $b \neq 0$, the center of each cluster does not pass through the center of the other component where the potential is the deepest. This means, each particle experiences a smaller potential variation than the case with $b = 0$. Since the energy-conversion efficiency from the bulk motion to the internal motion depends critically on the potential changes (Eq. (7)), the relaxation times are systematically longer when $b \neq 0$, compared with the models with $b = 0$. Therefore, a head-on collision yields a shorter relaxation time than an offcenter collision. The possibility of non-zero impact parameter in real cluster collision (Fabian & Daines 1991) strengthens our conclusion mentioned in Sec.3.4.

4. Discussion and conclusion

We have performed N-body simulations to study the relaxation process of two, equal-mass colliding subcluster of galaxies. We have demonstrated that it is difficult to erase the bimodal structures in the dark matter distributions at the first encounter and that it remains for a long pe-

riod after the first encounter. Our results demonstrate that the rebounce time (hence the relaxation time) depends on the precise density and velocity distribution of the DM. There are two key parameters for the density profile, the core radius and the power index of the DM distribution in the outer region. We find that a smaller core radius or a steeper DM distribution yields a quicker relaxation. This is understood as the result of violent relaxation, in which a more efficient energy conversion from the relative motion to the internal motion occurs when the potential is steeper; namely, when a core radius is smaller and the density distribution is steeper. Our results show that it takes more than $4h$ times longer than the time scale assumed by RLT to erase substructures in the clusters after the first encounter even in the most quick merging cases, if the cluster collapsed later than a redshift of 1.
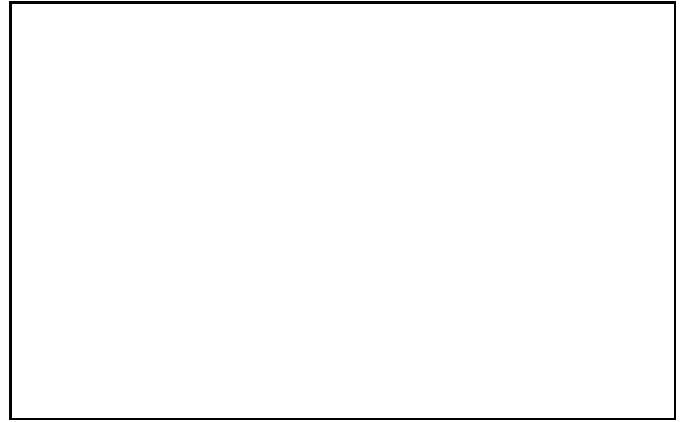
Fig. 8. Relation between Ω_0 and δt for various values of $\delta\tilde{F}$, the fraction of clusters formed between $T_0 - \delta t$ and T_0 with T_0 being the present age of the universe (cf. RLT).

This large merging time scale results in an appreciable decrease in the lower limit of Ω_0. Figure 8 displays the relation between Ω_0 and δt for various values of $\delta\tilde{F}$, which represents the fraction of clusters formed between $T_0 - \delta t$ and T_0, where T_0 is the present age of the Universe (cf. RLT). We find an approximate fitting formula from Fig. 8

$$\Omega_0 \gtrsim \frac{0.32\delta\tilde{F}}{\delta t/T_0(\Omega_0, \lambda_0)} \tag{8}$$

for $0.25 \lesssim \delta\tilde{F} \lesssim 0.40$ and $0.0 \leq \delta t/T_0 \lesssim 0.6$. Numerically solving Eq. (8) for Ω_0 yields an approximate formula,

$$\Omega_0 \gtrsim \frac{0.26\delta\tilde{F}}{\delta t \, H_0}, \tag{9}$$

which is almost independent on λ_0. It shows that the derived lower limit of Ω_0 is strongly depending on the assumed relaxation time. RLT took $\delta\tilde{F} \gtrsim 0.25$ mainly from

observed X-ray surface brightness contours by Jones & Forman(1990) and derived $\Omega_0 \gtrsim 0.5$ for $\delta t \lesssim 0.1 H_0^{-1}$. Our simulations demonstrate that the rebounce timescale is $t_{\rm reb}/t_{\rm RLT} \sim 4 - 10h$, where $t_{\rm RLT} = 10^9 h^{-1}{\rm yr}$ is merging timescale adopted by RLT. Since the relaxation time is longer than the rebounce timescale, we have

$$\delta t \gtrsim t_{\rm reb} \simeq (4 - 10) \times 10^9 {\rm yr}, \tag{10}$$

as the relaxation time of the DM distribution. If the gas always follows the DM distribution, we can apply this result to estimate the lower limit of Ω_0 with this substructure frequency deduced from X-ray observations. It shows that even if $\delta t = t_{\rm reb}$, the derived lower limit of the density of the universe is more than a factor of 2 smaller than the value derived by RLT as

$$\Omega_0 \gtrsim 0.18 \Big(\frac{t_{\rm reb}/t_{\rm RLT}}{4.0}\Big)^{-1}. \tag{11}$$

If we take into account the fact that the oscillatory motion of merging substructures still survives after the second encounter and that the adopted value is obtained by using the model with an extremely centrally concentrated mass distribution which leads to the shortest relaxation time, the true relaxation time could be longer than this and a much lower density universe could be consistent with the observed substructure frequency.

Finally, we would like to note the applicability of our present results to the estimation of the mean density of the universe based on the statistics of the appearance of the substructures in clusters. In the above discussion, we have assumed that the morphology of the X-ray emitting gas always follows the morphology of the dark matter distributions. However, it is still unclear whether the hot gas follows the DM or not. There is evidence which supports this assumption both in simulations (Roettiger et al. 1993) and in the real world (Briel et al. 1992). Roettiger et al. (1993) have shown that even after the encounter of two clusters the X-ray emitting gas almost traces the dark matter distributions and they have suggested that the substructure in the Coma cluster found by X-ray morphology (Briel et al. 1992) is in this post encounter stage. However, there is also a counter evidence against this assumption in simulations (Evrard 1990; Schindler & Müller 1993) where the bimodal structure of the X-ray emitting gas disappears when two substructures meet although the dark matter of the two substructures passes through each other (Evrard 1990; Schindler & Böhringer 1993). Probably the both cases are occurring in real clusters depending on their merging conditions but it is not sure which is the dominant process. If the fraction of merger events represented by the former case is dominant, we can safely assume the above mentioned assumption. However, if the fraction of the merging events represented by the latter case is dominant, the frequency of substructures in dark matter distribution deduced from X-ray data is highly underestimated. Fortunately, there is now a new useful tool

to study the dark matter distribution in clusters directly, that is gravitational lensing technique (e.g. Fort & Mellier 1994). If the latter is the case, we will find a large discrepancy of substructure frequency between the results deduced by the gravitational lensing technique and the X-ray data, that is the former will be much higher. This will be a good test which of above two processes is dominant process in real world.

The special nature of the initial conditions in our simulations would also limit the applicability of our results to the real cluster merging. There have been extensive N-body calculations based on somewhat more cosmologically motivated initial conditions than are the present calculations (e.g. Evrard et al. 1993; Crone, Evrard & Richstone 1994;Jing et al. 1994). Although their approaches are basically more straightforward to compare their results with real cluster observations, their present results are still largely limited by their numerical resolution, size of the simulation boxes, number of the simulated samples, baryon fraction, and so on. Actually, the results obtained by this approach are still controversial. Jing et al. (1994) have obtained much a larger fraction of clusters having substructures in a low density universe than Evrard et al. (1993) who found that the morphology of clusters in low-density universes are much more regular, spherically symmetric than those in the critical density universe. In this situation, our approach has a complementary meaning to examine the cluster merging process. Our present study is enough to make a caution to require recent cluster formation to explain the high fraction of nearby clusters having substructures and to conclude that the density of the universe prefers to be high by using RLT's method.

In conclusion, the result of a high density universe RLT derived should be still in question because multiple X-ray clusters cannot be easily considered as evidence for recent cluster formation according to our simulation results. Further studies to clarify the dependence on the relaxation timescale is required.

References

Bahcall N. A., 1975, ApJ 198, 249
Bartelmann M.,Ehlers J.,Schneider P., 1993, A&A 280, 351

Briel U. G.,Henry J. P.,Schwarz R. A. et al., 1991, A&A 246 L10

Briel U. G.,Henry J. P.,Bóhringer H.,1992, A&A 259,L31

Cavaliere A.,Fasco-Femiano R., 1976, A&A 49, 137

Crone M. M.,Evrard A. E.,Richstone D. O., 1994,ApJ *in press*

Dressler A.,Shectman S. A,1988, AJ 95, 985

Evrard A. E., 1990, ApJ 363,349

Evrard A. E.,Mohr J. J.,Fabricant D. G.,Geller M. J., 1993, ApJ 419, L9

Fabian A. C.,Daines S. J., 1991 , MNRAS 252,17

Fitchett M. J., 1990, in: Clusters of Galaxies,Oegerle W. R., Fitchett M. J., Danly L.(eds.). Cambridge Univ. Press,Cambridge,p111

Fort B.,Mellier Y., 1994, AAR 5, 239

Funato Y.,Makino J.,Ebisuzaki T., 1992, PASJ 44,291

Geller M. J.,Beers T. C., 1982, PASP 94, 421

Hammer F.,1991, ApJ 383, 66

Henry J. P.,Briel U. G.,Nulsen P. E. J., 1993, A&A 271, 413

Hughes J. P., 1989, ApJ 337, 21

Jing Y. P.,Mo H. J.,Börner G.,Fang L. Z., 1994, preprint

Jones C.,Forman W., 1990, in:Clusters of Galaxies,Oegerle W. R., Fitchett M. J., Danly L.(eds.).Cambridge Univ. Press , Cambridge, p.257

Kaiser N., 1986, MNRAS 222, 323

King R. I., 1972, AJ 174, L123

LeFavre et al.,1994, ApJ 422, L5

Lynden-Bell D., 1967, MNRAS 136, 101

McGlynn T. A.,Fabian A. C., 1984, MNRAS 208, 709 (MF)

Miralda-Escudé J., 1991,Ph.D.Thesis, Princeton University

Miralda-Escudé J.,Babul,A.,1994, preprint

Ponman T. J.,Watt M. P.,Bertram D. et al., 1992, in: Frontiers of X-ray astronomy,Tanaka Y., Koyama K.(eds.). University Academy Press, Tokyo, p.467

Richstone D.,Loeb A.,Turner E. L., 1992, ApJ 393, 477 (RLT)

Roettiger K.,Burns J.,Loken C., 1993, ApJ 407, L53

Sarazin C. L., 1988, X-ray emission from clusters of galaxies, Cambridge Univ. Press, Cambridge

Schindler S.,Böhringer H.,1993, A&A 269, 83

Schindler S.,Müller, 1993, A&A

Tully R. B., 1987, ApJ 321, 280

White S. D. M.,Navarro J. F.,Evrard A. E.,Frenk C. S., 1993, Nat 366, 429

Wu X.,Hammer F., 1993, MNRAS 262, 187

Wu X., 1994, preprint

Yoshii Y.,Takahara F., 1989, ApJ 346, 28